Supplement of Biogeosciences, 20, 4391–4412, 2023
https://doi.org/10.5194/bg-20-4391-2023-supplement

Biogeosciences Open Access EGU

Supplement of

Changes in biogenic volatile organic compound emissions in response to the El Niño–Southern Oscillation

Ryan Vella et al.

Correspondence to: Ryan Vella (ryan.vella@mpic.de)

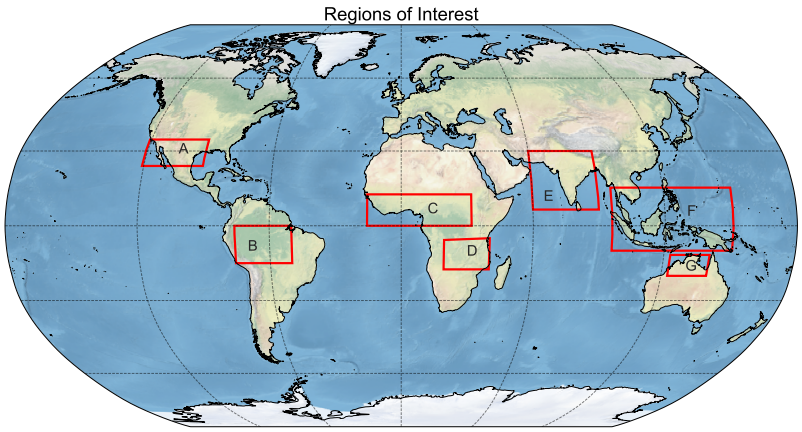

Figure S1. Regions of interest. The extent of areas is presented in Table 1.

Region	Label on figures	Acronym	Latitude range	Longitude range
South West USA	A	SWUSA	24, 34.6	-120.8, -92.4
Amazon Basin	B	Amazon	-15, 0	-75.8, -50
Central West Africa	C	CEAfr	0, 12.6	-15.54, 32
South East Africa	D	SEAfr	-14.6, -5.7	19.5, 40.3
India	E	India	6.5, 30	60, 90
South East Asia	F	SEAsia	-10, 15.3	96, 151
North Australia.	G	NAus	-20.1, -11.7	123, 141

Table S1. Details on the regions considered.

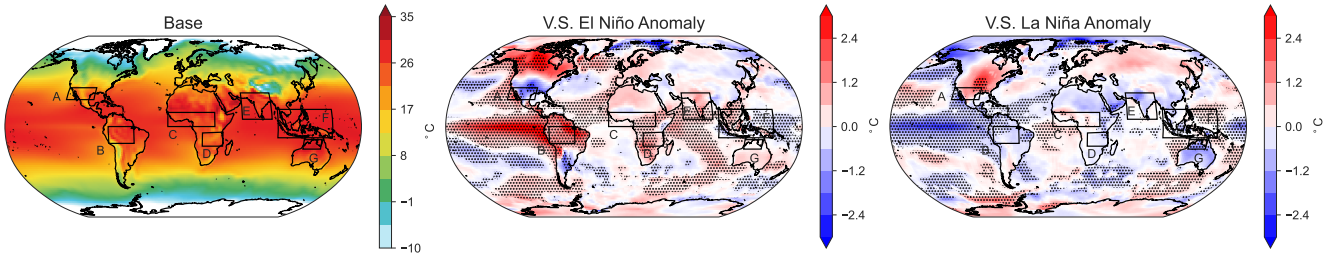

Figure S2. Same plot for surface temperature as in Fig. 4 but also showing anomalies over the ocean. This confirms that our model captures well the ENSO scenarios.

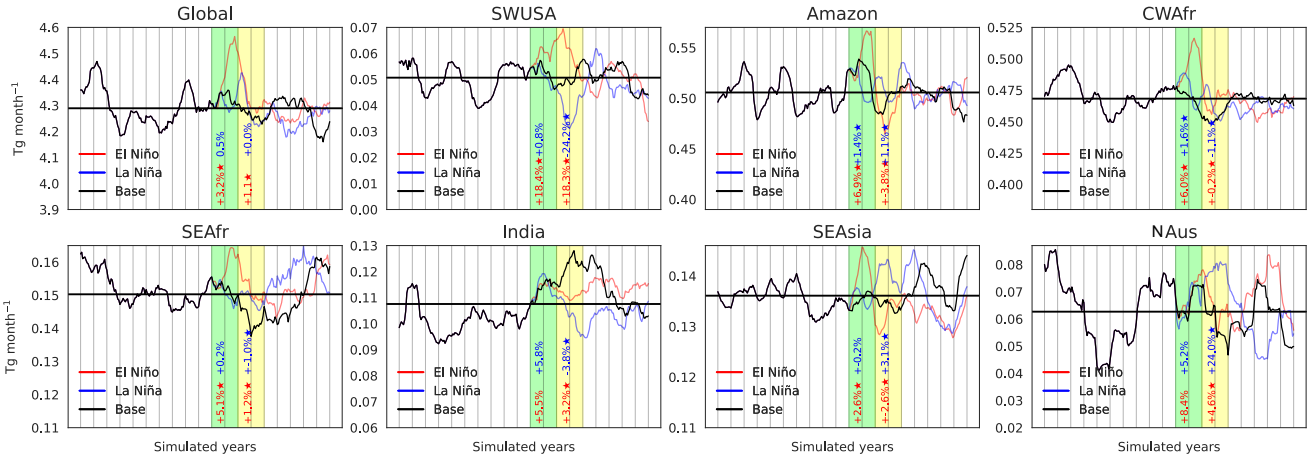

Figure S3. Time evolution of global and regional monoterpene fluxes with El Niño (red) and La Niña (blue) events over two years (green columns). The black line illustrates base conditions throughout all simulations. Statistically significant changes (p<.01) are marked with a star.

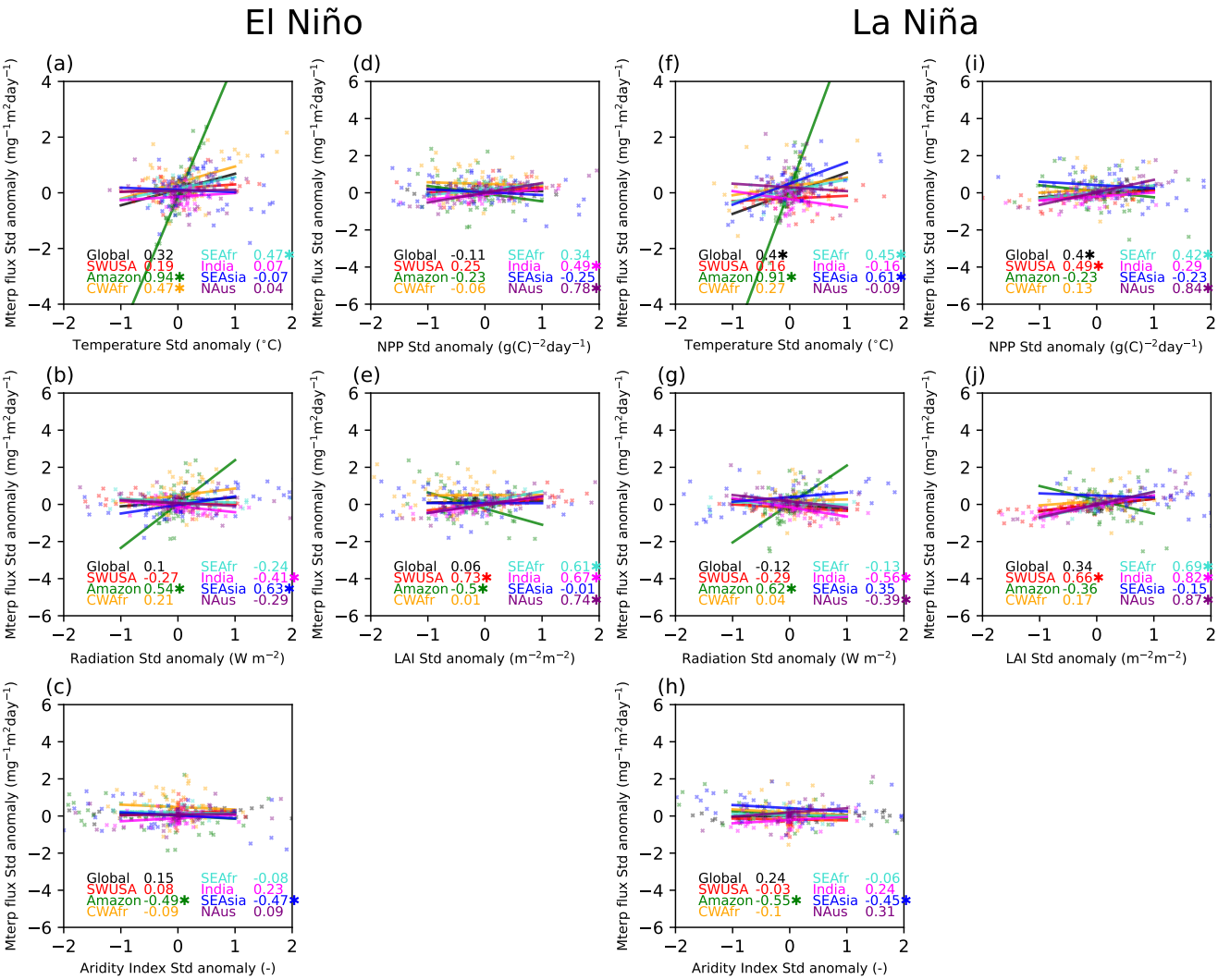

Figure S4. Scatter plots with a linear regression fit including the Pearson's correlation (r) between the standardized monoterpene flux anomaly and standardized temperature, radiation, AI, NPP, and LAI anomaly at different regions for the event years and the following two years (four years in total). Very strong El Niño and La Niña events are shown in the top and bottom panels, respectively.

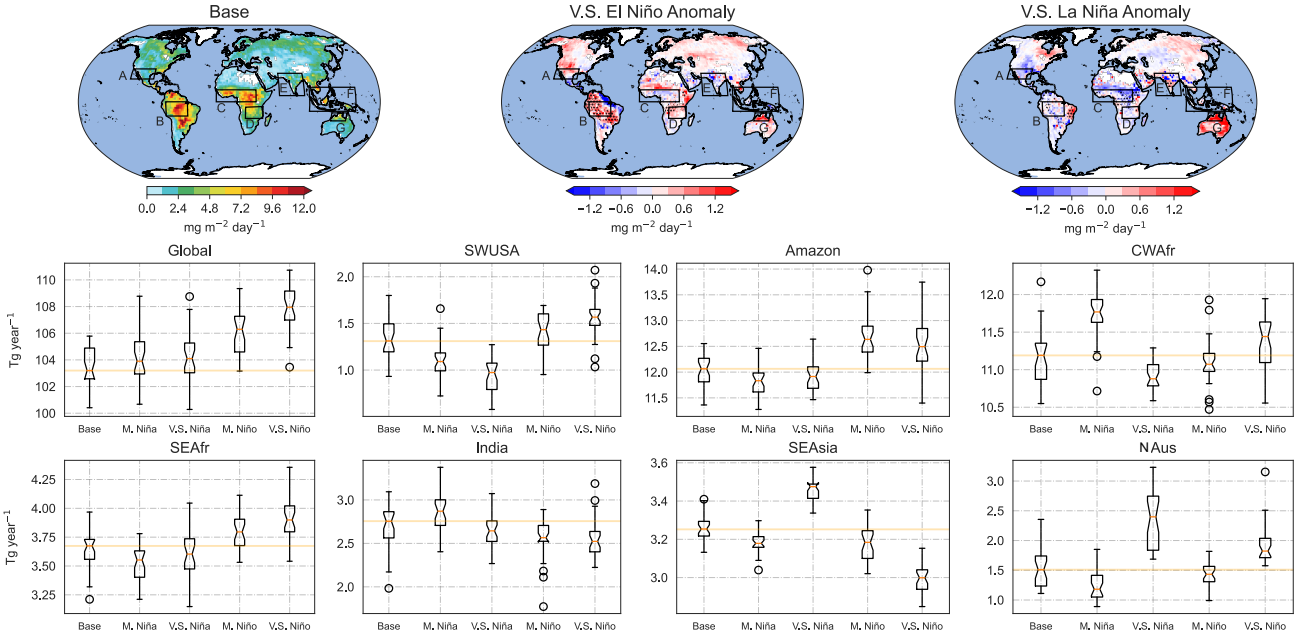

Figure S5. Global monoterpene fluxes for the base scenarios as well as changes in emissions during very strong El Niño and La Niña events. The bar plots show emission changes for the different scenarios. The median of the base scenario is indicated in orange.

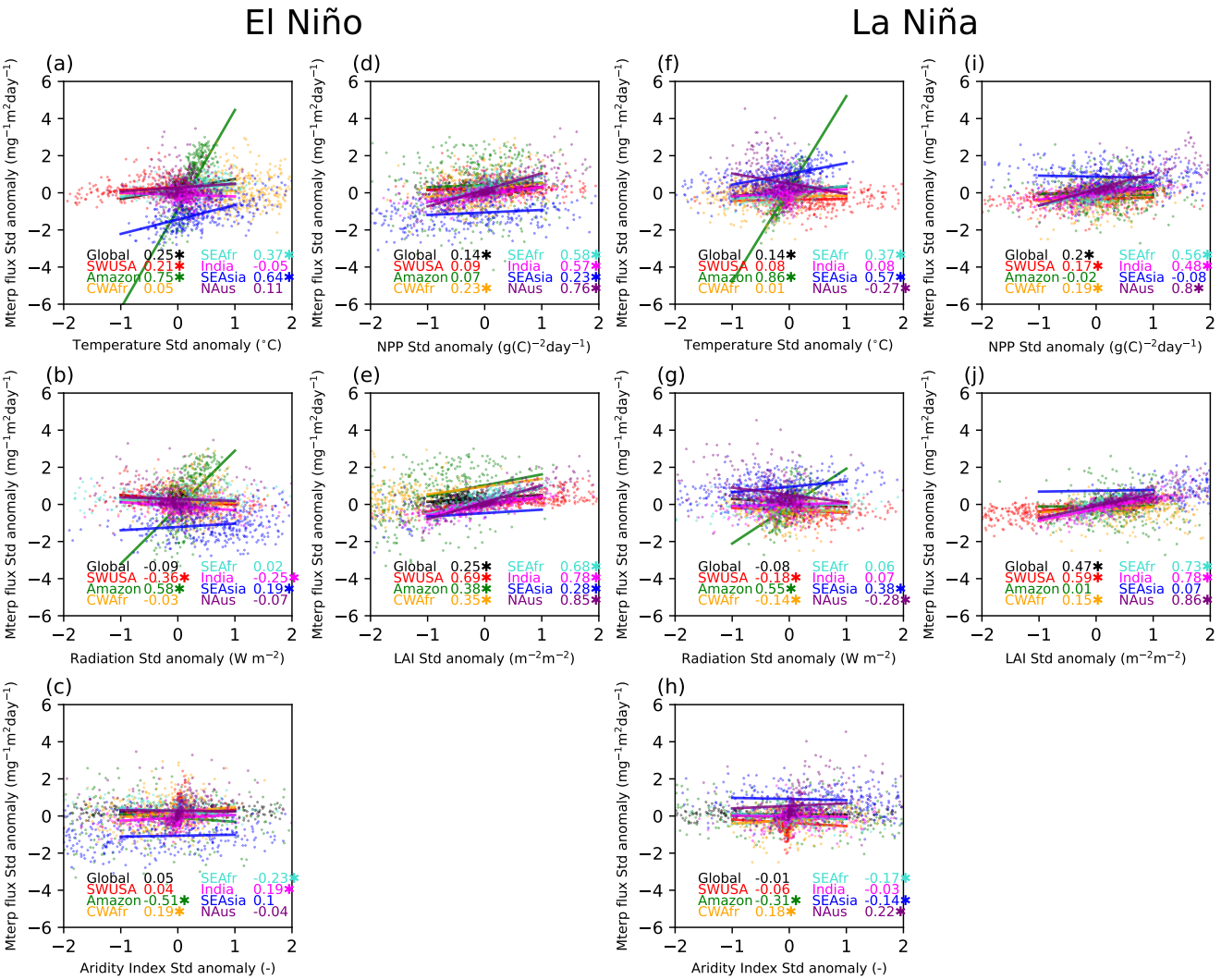

Figure S6. Scatter plots with a linear regression fit including the Pearson's correlation (r) between the standardized monoterpene flux anomaly and standardized temperature, radiation, AI, NPP, and LAI anomaly at different regions for very strong El Niño (top panels) and La Niña (bottom panels) events. Correlations with p<.01 are marked with a star.

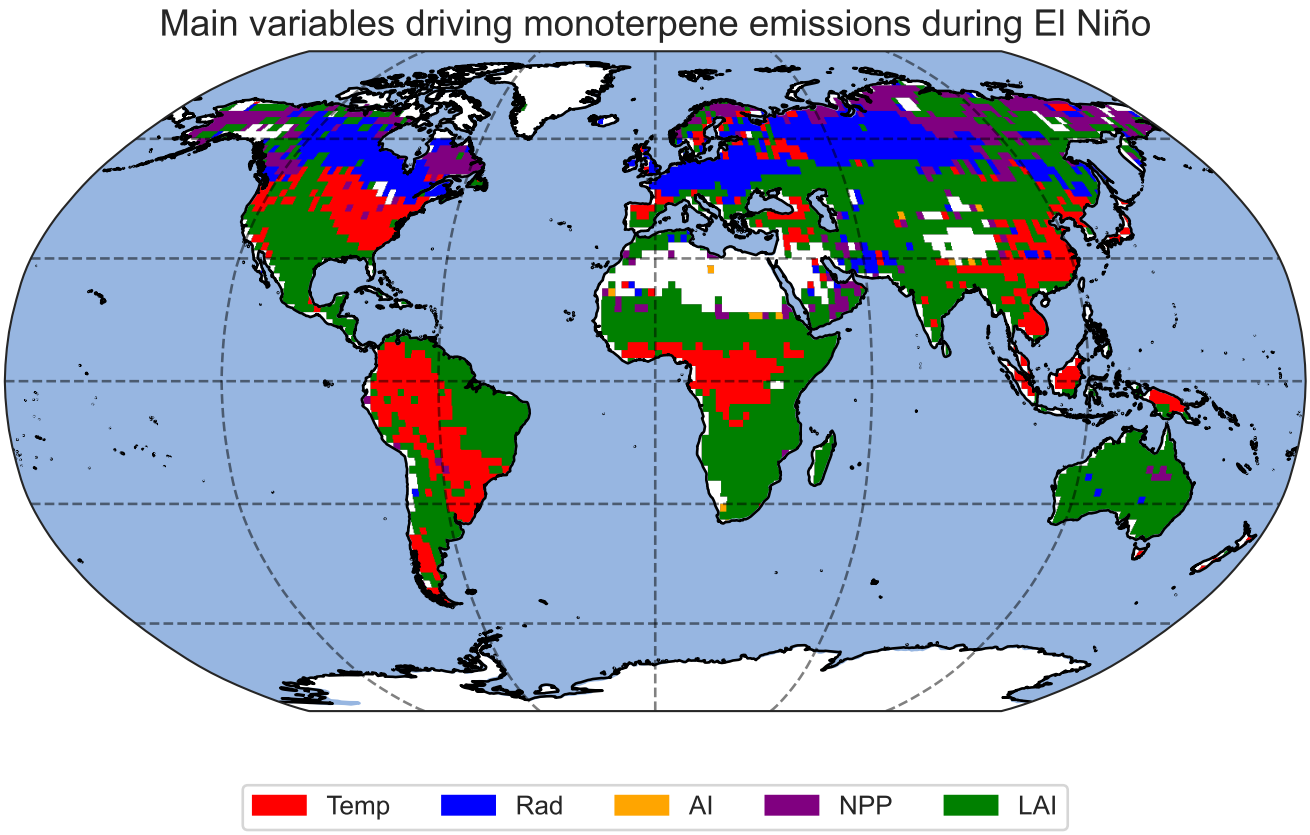

Figure S7. Map showing the variables whose anomalies correlate most strongly with the monoterpene flux change for every pixel of the model output. The correlations between the monoterpene flux and the temperature, radiation, AI, NPP, and LAI anomalies are classified using PCA.